



Synergistic effect of arsenic removal from petroleum condensate via liquid-liquid extraction: Thermodynamics, kinetics, DFT and McCabe-Thiele method

Kittamuk Purktimatanont^a, Vanee Mohdee^a, Ura Pancharoen^{a,*},
Kreangkrai Maneeintr^{b,**}, Wikorn Punyain^{c,***}, Anchaleeporn W. Lothongkum^d

^a Department of Chemical Engineering, Faculty of Engineering, Chulalongkorn University, Bangkok, 10330, Thailand

^b Carbon Capture, Storage and Utilization Research Group, Department of Mining and, Petroleum Engineering, Faculty of Engineering, Chulalongkorn University, Bangkok, 10330, Thailand

^c Department of Chemistry and Center of Excellence in Biomaterials, Faculty of Science, Naresuan University, Phitsanulok, 65000, Thailand

^d Department of Chemical Engineering, School of Engineering, King Mongkut's Institute of Technology Ladkrabang, Ladkrabang, Bangkok, 10520, Thailand

ARTICLE INFO

Keywords:

Arsenic
Petroleum condensate
Liquid-liquid extraction
Box-behnken design
McCabe-thiele
Density functional theory

ABSTRACT

This work presents the purification of petroleum condensate by removing arsenic ions via liquid-liquid extraction (LLE). Influence of pure and synergistic extractants is investigated. In terms of the practicability, following parameters are examined: the type of extractant, operating time, and temperature. Response surface methodology is used to design parameters such as organic-aqueous ratio and extractant concentration. Under optimal conditions; a mixture of 1 mol/L HCl and 0.02 mol/L thiourea with an organic/aqueous ratio of 1:4 at 323.15 K for 60 min, the extraction of arsenic reached 78.2 %. Further, batch simulation via two-stage counter-current extraction, and estimation by McCabe-Thiele diagram proved to be enhanced arsenic extraction to 95.3 %. Analysis by FTIR show that arsenic ions in petroleum condensate are formed as triphenylarsine compound ((C₆H₅)₃As). The process of arsenic removal proved to be zero-order endothermic, irreversible and spontaneous reaction. The results obtained from the density functional theory (DFT) confirm that arsenic ions react with the synergistic extractant: effectively forming a covalent bond (As-S).

1. Introduction

Petroleum and natural gas condensates from offshore oil and gas production is always contaminated with arsenic. Petroleum and natural gas condensates are liquid hydrocarbons condensed from the gas phase in both oil and gas wells. The carbon number of hydrocarbon compounds in petroleum condensates range from 2 to 25. Condensates are an important raw material for the refinery and petrochemical industry i.e. a diluent for heavy crudes, refinery and blending feedstock for further transformation, and petrochemical feedstock for steam crackers [1,2]. Upstream condensates contain an over-limiting concentration of arsenic. In general, various forms

* Corresponding author.

** Corresponding author.

*** Corresponding author.

E-mail addresses: ura.p@chula.ac.th (U. Pancharoen), kreangkrai.m@chula.ac.th (K. Maneeintr), kraiwanp@nu.ac.th (W. Punyain).

of arsenic contaminated in condensates can be found: namely, trimethylarsine or TMA ((CH₃)₃As), triethylarsine ((C₂H₅)₃As), triphenylarsine ((C₆H₅)₃As), and arsine (AsH₃) in the range of 0.04–514 mg/L depending on the oil and gas wells [3,4]. Arsenic is a highly poisonous metal and can cause chronic and acute poisoning in humans [5]. Arsenic can also contribute to permanent catalyst poisoning and corrosion of equipment in the refinery and petrochemical processes. It is reported that the concentration of arsenic in thermal cracking of gasoline used directly into the furnace should be less than 0.01 mg/L [6–8]. It is crucial, therefore, that arsenic be removed from upstream condensates.

It is noted that investigations regarding the removal of arsenic ions from petroleum condensate, though highly important, are sparse and have rarely been found. Ichikawa et al. [9] applied adsorbents comprising coconut husk activated carbon, bituminous coal and organic polymeric compounds (polystyrene-type polymer) in the adsorption process to remove arsenic from petroleum fractions. It is seen that arsenic could be adsorbed from light naphtha containing 220 ppb of arsenic >99%. In the preparation of adsorbents, there are many steps and temperature must be controlled. Chaturabul et al. [4] separated arsenic from natural gas condensate using hydrochloric acid and methanol as an extractant via a pulsed sieve plate column. Thus, arsenic removal reached 94% with 0.02 m/s pulse velocity and a volumetric flow rate ratio of the condensate to the extractant of 1:4. However, the pulsed sieve plate column consumed a large amount of the extractant.

Liquid-liquid extraction (LLE) is a separation technique associated with two immiscible or partially miscible liquids used to separate compounds. LLE has been successfully applied in many industrial applications such as removing antibiotics from foodstuff, removing antibiotics in the pharmaceutical industry and separating rare earth elements and diverse types of metal ions [10–15]. In Table 1, the advantages and disadvantages of various separation techniques are shown [16–18].

In the LLE process, the McCabe-Thiele graphical method has been widely applied to determine the number of extraction stages for the required concentration [19,20]. Yao et al. [20] applied the McCabe-Thiele method to eliminate chloride from wastewater by predicting the effective stages of extraction and stripping via LLE process. The effective stages of extraction and stripping were found to be two and three stages, respectively. The final chloride content in wastewater less than 350 mg/L and stripping percentage of 99 were confirmed by a batch simulated counter-current operation. The McCabe-Thiele method has proved to be a useful tool for use in the separation and purification processes [19].

In the LLE process, both kinetics and thermodynamics play a key role. Kinetic studies are seen to expose the mechanisms of diffusion and chemical reaction in the extraction process. Kinetics provide important data such as residence time and reagent concentration [21,22]. Thermodynamic studies have also been used to study the energy changes in reactions and provide data for the energy design of the processes involved with the reactions [23,24]. In addition, density functional theory (DFT) is a chemistry tool for molecular charge density and its electronic properties to describe complex electronic structures [25,26]. Furthermore, DFT can be used to analyze the extraction process of arsenic as well as arsenic ions [27]. Becke's 3-parameter Lee Yang Parr (B3LYP) functional is a hybrid of several components, which can successfully describe various characteristics over a wide range of systems [28,29]. Sun et al. [30] applied DFT to understand reaction mechanisms as well as to calculate the atomic electronegativity of different diluents in the lithium extraction process. Thus, both subjects are important factors in diluent selection. Khan et al. [31] used DFT to calculate the interaction energy between DCH18C6-HTcO₄ and DCH18C6-HNO₃ to compare and identify key factors in technetium extraction.

The novelty of this work is the removal of arsenic from petroleum condensate via LLE using synergistic extractant. The arsenic compound in petroleum condensate is identified by Fourier-transform infrared spectroscopy (FTIR). The types of extractants investigated are based on extractants and stripping solutions which are aqueous solutions in previous studies, as shown in Table 2 [4,7, 32–36]. Response Surface Methodology (RSM) based on Box-Behnken design (BBD) is employed to optimize the operating condition such as concentration of extractant and O/A ratio. Operating time and temperature are further investigated to improve the efficiency of the LLE system. The multistage extraction is carried out to increase the removal performance. A batch simulation of counter-current extraction is used to confirm the prediction of the arsenic concentration by McCabe-Thiele diagrams. Furthermore, an understanding of the system has been examined via the kinetic study and the thermodynamic study. Finally, understanding the molecular interactions and mechanisms of extraction processes is simulated by DFT.

Table 1
Advantages and disadvantages of batch separation techniques.

Techniques	Advantages	Disadvantages
Adsorption	- High efficiency - Simple system installation	- High capital costs - Adsorbents deterioration - Require adsorbents regeneration
Ion-exchange	- High efficiency - Simple equipment and operation - Easy preparation - No mixing required	- High capital costs - Specific application for charged molecules - Require feed prefiltration - Slow process
Liquid membrane	- Extraction and stripping in a single stage - Low capital costs	- Leak of liquid membrane (instability) - Low efficiency
Liquid-liquid extraction	- High efficiency - High selectivity - Various applications - Simple equipment and operation	- Require time for phase separation - Solvent loss

Table 2
Summary of previous studies for arsenic separation.

Authors	Feeds	Extractants	Stripping solutions	Processes	Extraction efficiency	Stripping efficiency
Chaturabul et al. [4]	Natural gas condensate	Methanol + HCl (Aq)	–	PSPC	94 %	–
Mohdee et al. [7]	Petroleum produced water	Aliquat 336 + Cyanex 921 (Org)	Thiourea + HCl (Aq)	HFMC	94 %	78 %
Wisniewski et al. [32]	Sulfuric acid solutions	Cyanex 923 (Org)	H ₂ O (Aq)	LLE	63 %	–
Pancharoen et al. [33]	Synthetic produced water	Aliquat 336 (Org)	NaOH (Aq)	HFSLM	91 %	72 %
Jantunen et al. [34]	Concentrated sulfuric acid	TBP (Org)	H ₂ O (Aq)	LLE	83 %	89 %
Suren et al. [35]	Synthetic produced water	Aliquat 336 (Org)	Thiourea + HCl (Aq)	HFSLM	99 %	98 %
Zeng et al. [36]	Hydrochloric acid	2-Ethylhexanol (Org)	HCl (Aq)	LLE	97 %	97 %

Note: (org) = organic phase, (aq) = aqueous phase, LLE = liquid-liquid extraction, HFSLM = hollow fiber supported liquid membrane, HFMC = hollow fiber membrane contactor, and PSPC = pulsed sieve plate column.

2. Materials and methods

2.1. Chemicals

Sodium hydroxide (98 % purity), sodium chloride (99.5 % purity) and thiourea (99 % purity) were purchased from Loba Chemie, India. Sulfuric acid (98 % purity) and hydrochloric acid (37 % purity) were bought from Qrec, New Zealand. Nitric acid (65 % purity) was obtained from Merck, Singapore. Methanol (99 % purity) was obtained from Fisher Scientific, United Kingdom. Petroleum condensate from the oil and gas plant in Greater Bongkot area, North Thailand was provided by Verasuwan Co., Ltd. Table 3 presented the composition of various metal ions contaminant in condensate sample.

2.2. Apparatus

Temperature and stirring speed were controlled using a digital hotplate stirrer (Stuart UC152D). Accuracy of the temperature was confirmed using mercury thermometer (± 274.15 K). Arsenic concentration was analyzed by atomic absorption spectrophotometer (AAS) (Varian/AA240FS). Fourier-transform infrared spectroscopy (FTIR) (Perkin Eimer/Spectrum One) was used to identify functional groups and changes in chemical bonding.

2.3. Experimental procedures

2.3.1. Extraction process

As shown in Fig. 1, the LLE process was used in the extraction of arsenic from petroleum condensate by implementing atmospheric pressure and temperature (313.15 K) with O/A equal to 1, stirring speed of 500 rpm via a magnetic bar with a digital hotplate stirrer for 60 min in a closed system. Firstly, NaOH, H₂SO₄, HNO₃, HCl, NH₂CSNH₂, and CH₃OH as potential extractants was carried out for pure extractant system. All extractants were applied at a concentration of 0.5 mol/L; the effective extractant will be employed in the following experiment (Response surface methodology (RSM), McCabe-Thiele plots, batch simulations, kinetics, and thermodynamics). Besides, the synergistic extractants also evaluated as follows; HCl + HNO₃, HCl + CH₃OH and HCl + NH₂CSNH₂.

2.3.2. Design of experiment

RSM along with Box-Behnken design (BBD) was used to design the experiment whereby both synergistic extractant concentration and O/A ratio were used. In Table 4, three levels, (−1, 0, 1), of 3 independent variables were studied in this work.

For this purpose, BBD is an effective tool for optimizing the extraction process and is used to fit the mathematical model that can demonstrate the predicted percentage of the extraction [37,38]. The following equation presents a quadratic polynomial model, which

Table 3
Compositions of the contaminants in petroleum condensate used in this work.

Metals	Concentration (mg/L)	Technique
Arsenic	0.050–2.100	ICP-MS
Mercury	0.065–2.400	ASTM UOP938
Zinc	<1.000	ICP-ES
Nickel	<1.000	ICP-ES

Note: ICP-MS = inductively coupled plasma-mass spectrometry, ASTM UOP938 = Total mercury and mercury species in liquid hydrocarbon, and ICP-ES = inductively coupled plasma-emission spectrometry.

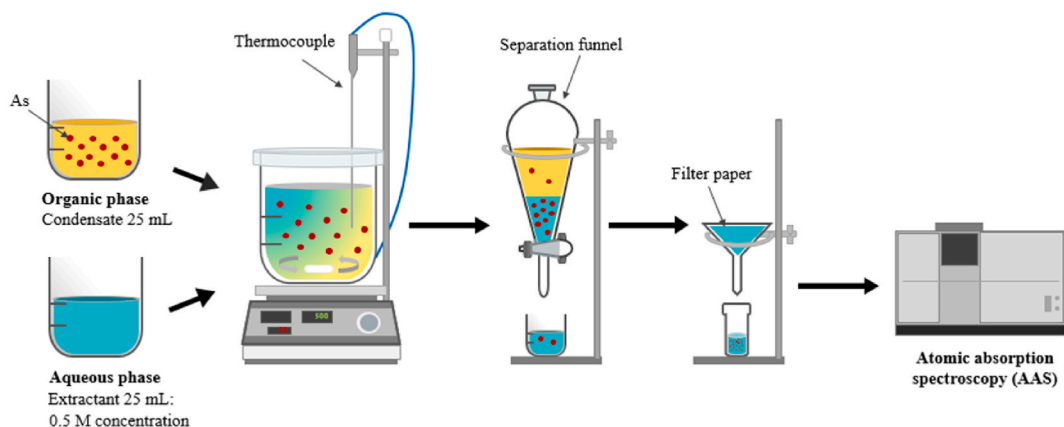


Fig. 1. Schematic illustration of liquid-liquid extraction for arsenic removal.

Table 4
Range of independent parameters.

X_i	-1	0	1
X_1 (HCl concentration)	0.5	1.5	2.5
X_2 (thiourea concentration)	0.01	0.13	0.25
X_3 (O/A ratio)	0.5	2.25	4

is able to predict extraction percentage [39], as shown in Eq. (1) [40]:

$$Y = \beta_0 + \sum_{i=1}^k \beta_i X_i + \sum_{i=1}^k \beta_{ii} X_i^2 + \sum_{i=1}^{k-1} \sum_{j=i+1}^k \beta_{ij} X_i X_j \quad (1)$$

where Y is the predicted response, β_0 is constant, β_i , β_{ii} and β_{ij} are the linear, quadratic, and interaction coefficients, respectively. X_i and X_j are the values of the independent parameters.

2.3.3. Batch simulation of two-stage counter-current extraction

In Fig. 2(a) and (b), the experiment to simulate the concentration of arsenic between two stages is shown. In the first stage (E1-1), petroleum condensate was mixed with the extractant. In the second stage (E2-1), petroleum condensate was mixed with the fresh extractant. Further, the extractant in the second stage was mixed with new petroleum condensate in the first stage (E1-2). The experiment was repeated until steady stage was reached, where arsenic concentration in the final stage was equal to the previous stage of petroleum condensate (C1) and the extractant (E2).

2.4. Analyses

The concentration of arsenic ions was analyzed using an atomic absorption spectrometer (AAS) for both the aqueous and organic phases. Fourier-transform infrared spectroscopy (FTIR) was also applied to evaluate the functional groups.

Percentage calculation of extraction and distribution ratio can be expressed as follows [41]:

$$\% \text{ Extraction} = \frac{C_{Aq,t}}{C_{Org,0}} \cdot 100\% \quad (2)$$

$$D) = \frac{C_{Aq,t}}{C_{Org,t}} \quad (3)$$

where $C_{Aq,t}$ is the concentration of arsenic after the extraction process in the aqueous phase, $C_{Org,t}$ is the concentration of arsenic after the extraction process in the organic phase and $C_{Org,0}$ is the concentration of arsenic before the extraction process in the organic phase.

Synergistic coefficients (S) were used to evaluate the effect of the synergistic solution. The value of $S > 1$ signifies the synergism of the synergistic solution; the value of $S < 1$ indicates the antagonism of the synergistic solution [7]. Synergistic coefficients (S) can be calculated as shown [41]:

$$S = \frac{D_{AB}}{D_A + D_B} \quad (4)$$

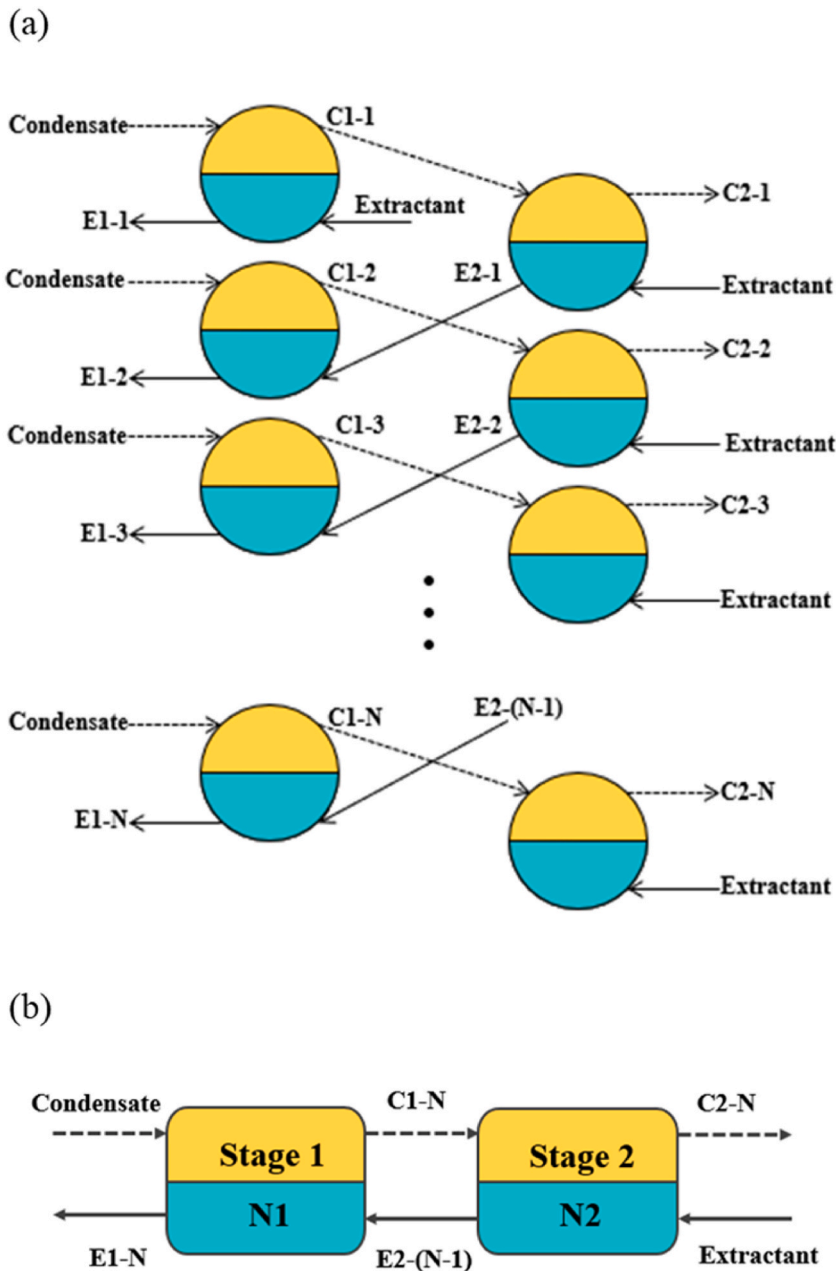


Fig. 2. (a) Batch simulation of the two-stage counter-current extraction of petroleum condensate with the synergistic extractant, and (b) Two-stage counter-current extraction process.

The separation factor (SF) represents the trend between metal ions and two species regards separation from each other in the LLE system. The separation factor (SF) can be calculated, accordingly [42]:

$$SF_{A,B} = \frac{D_A}{D_B} \tag{5}$$

2.5. Thermodynamics investigation

The Arrhenius equation is a mathematical expression explaining the result of the velocity of a chemical reaction's temperature [43, 44]. As shown in Eq. (6), the Arrhenius equation is the basis for all predictive expressions applied to calculate reaction-rate constants. After that, activation energy (E_a) was determined by plotting $\ln k$ versus $1/T$ and taking the natural logarithm as in Eq. (7):

$$k(T) = A e^{-\frac{E_a}{RT}} \quad (6)$$

$$\ln k = \ln A - \frac{E_a}{R} \left(\frac{1}{T} \right) \quad (7)$$

where k is a reaction rate constant, T is the temperature used in the system, A is a pre-exponential factor or a frequency factor, E_a is activation energy (J/mol), and R is the universal gas constant (8.314 J/mol·K).

Van't Hoff equation is an equation that estimates ΔH° , ΔS° and ΔG° , as in Eq. (8) by plotting a straight-line equation of $\ln K_{ex}$ versus $1/T$, given ΔH° from a slope and ΔS° from an intercept. After that, given ΔG° , and then substituting ΔH° and ΔS° in Eq. (9) yields [45, 46]:

$$\ln K_{ex} = -\frac{\Delta H^\circ}{RT} + \frac{\Delta S^\circ}{R} \quad (8)$$

$$\Delta G^\circ = \Delta H^\circ - T\Delta S^\circ \quad (9)$$

where ΔH° is standard enthalpy change, ΔS° is standard entropy change, and ΔG° is standard Gibbs free energy change. K_{ex} is the equilibrium constant.

2.6. Computational

DFT is used as a calculation tool in this work. The three-dimensional starting geometries for each molecule were constructed following the chemical reaction. Becke's 3-parameter Lee Yang Parr (B3LYP) functional with double zeta basis set cc-pVDZ was used in the geometry optimization process to find the optimized structures of each molecule, which play a role in the reaction mechanism. Solvent effects were considered using the conductor-like polarizable continuum model (CPCM): one of the most successful solvation models uses for calculations. Hessian calculations were carried out on the optimized geometries to confirm that the optimized geometries of each molecule are located on the local minimum of the potential energy surface (PES) and to analyze the vibrational frequencies. The calculated thermodynamics data were implemented at standard stage. All DFT calculations were done using the Gaussian09 program package [47]. Graphical molecular pictures were drawn by Avogadro [48], and IR spectra were plotted by the Gabedit [49] program package.

3. Results and discussion

3.1. FTIR spectroscopy of raw petroleum condensate

In Fig. 3, the species of arsenic in petroleum condensate is determined using FTIR spectra. The spectra of 2853.10–2954.79 cm^{-1} represent the alkane group, and the spectra of 1607.24–1746.76 cm^{-1} represent the aromatic compound [50]. Moreover, in the range

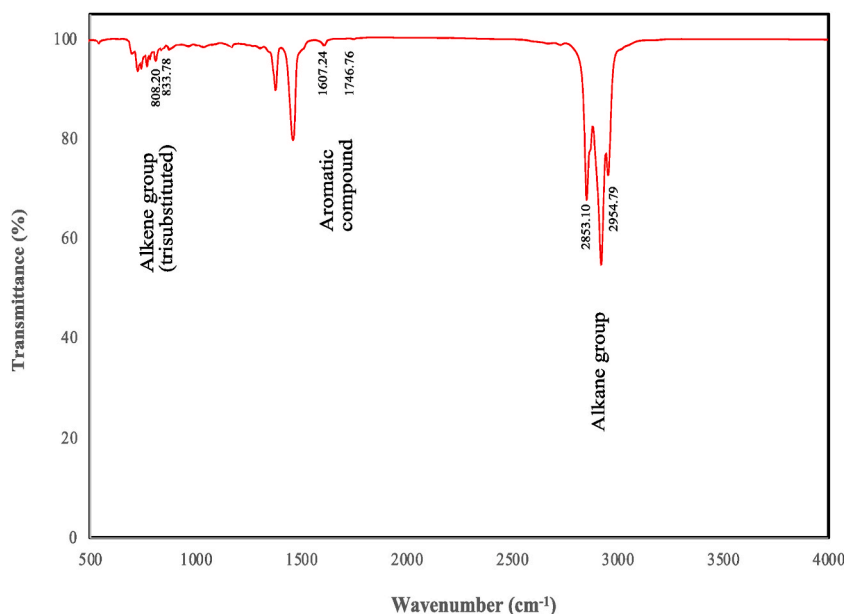


Fig. 3. FTIR spectra of petroleum condensate before extraction.

from 808.02 to 833.78 cm^{-1} , both the alkene group and the trisubstituted pattern are displayed [51], having more stability than the monosubstituted and disubstituted pattern [52]. It is evident, therefore, that the arsenic compound contained in the petroleum condensate was found to be triphenylarsine ((C_6H_5) $_3\text{As}$), which was in agreement with that obtained by Chaturabul et al. [4].

3.2. Types of extractants

To investigate the separation performance of arsenic: HCl, NaOH, HNO_3 , H_2SO_4 , CH_3OH , and NH_2CSNH_2 were used. In Fig. 4(a), HCl was found to provide the highest extraction percentage (16.7 %). However, pK_a values confirmed that HCl had the smallest value, resulting in high mass transport of HCl compared to other acids [53,54]. Thus, it is seen that the separation performance of the pure extractant was quite low, not sufficient for the removal of arsenic. Hence, many works have reported that synergistic solutions can enhance the separation efficiency of diverse type of metals separation [26]. Thereby, the synergistic effect is also carried out.

In Fig. 4(b), the mixture of 0.5 mol/L HCl and 0.5 mol/L (nitric acid, methanol, and thiourea) was used to improve the separation performance of arsenic. The mixture of HCl and thiourea reached 32.2 % arsenic extraction, resulting in a synergistic effect [55]. On the other hand, the mixture of HCl and methanol plus the mixture of HCl and nitric acid proved to be 12.8 % and 9.8 % of arsenic extraction, respectively. This outcome can be described by the bond-dissociation energy of the synergistic extractant. The reaction mechanism between HCl + Methanol and As occurred in the C–Cl bond (394.90 ± 13.40) [4,56]. Although, the reaction mechanism between HCl + Thiourea and As occurred in the H–S bond (353.57 ± 0.30) [56]. It is noted that the H–S bond had less bond-dissociation energy than the C–Cl bond, indicating less energy is required to break the bond.

In Table 5, the synergistic coefficient of the synergistic solution between HCl and Thiourea was >1 , confirming the synergism between HCl and Thiourea. In contrast, the synergistic solution between HCl and other solutions was <1 , confirming that the synergism was antagonistic. To compare the different synergistic solutions, Bond-dissociation energy needed to break the bond in the molecule [57].

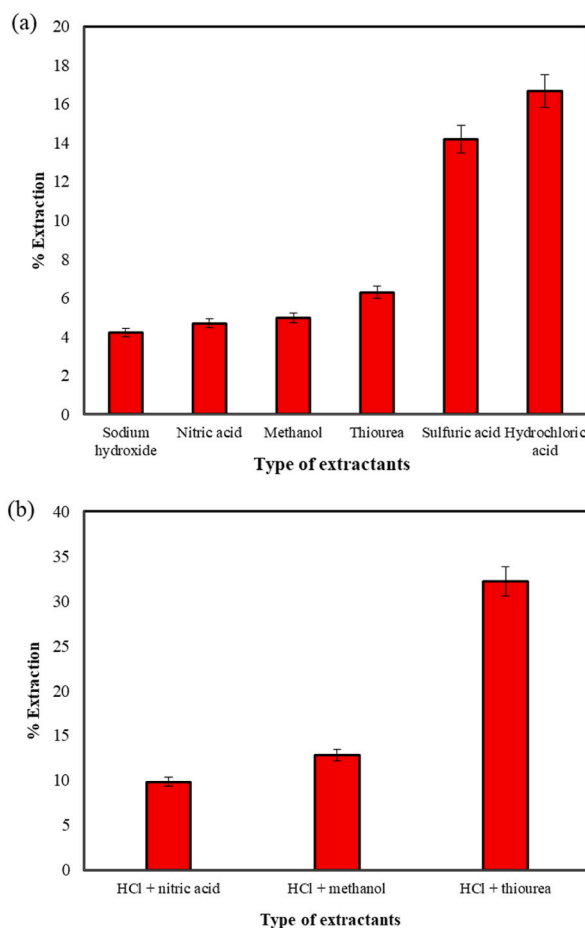


Fig. 4. (a) Percentages of extraction versus types of pure extractant, and (b) Percentages of extraction versus types of synthesis extractant under condition: 0.5 mol/L of each.

3.3. Concentration of synergistic extractants

The optimal concentration of synergistic extractants between HCl and thiourea was assessed via LLE methodology. In Fig. 5(a), thiourea concentrations varied from 0.05 to 1 mol/L, while HCl concentrations were fixed at 0.5 mol/L. The highest efficiency for the extraction of arsenic was achieved at 0.05 mol/L thiourea. In Fig. 5(b), the impact of HCl concentration on the extraction of arsenic is depicted. Since the concentration of HCl increased from 0.25 to 1 mol/L, the extraction performance of arsenic ions increased. This result is consistent with Le Chatelier's principle, whereby higher reactant concentration leads to the forward reaction [58]. The extraction performance reached a maximum of 1 mol/L HCl, achieving an extraction percentage of 43.3 %. Once HCl concentration passed over 1 mol/L, extraction percentage slightly decreased [35]. Therefore, both 0.05 mol/L thiourea concentration and 1 mol/L HCl concentration were used for further experiments.

3.4. Statistical analysis

3.4.1. Selection of investigated parameters

The three parameters, as seen in Table 4, were investigated for the extraction of arsenic ions. In Fig. 5, the concentrations of the synergistic reagents greatly affected the extractant percentage. Accordingly, at 1 mol/L HCl and 0.05 mol/L thiourea, the highest percentage of arsenic was obtained. Both HCl concentration and thiourea concentration were used as statistical parameters in the range from 0.5 to 2.5 mol/L HCl and 0.01–0.25 mol/L thiourea. Another statistical parameter: O/A ratio was chosen to study since O/A ratio is an operating line in the McCabe-Thiele diagram. O/A ratios are used in the range of 0.5–4.0 due to the efficiency of extraction processes [59].

3.4.2. Response surface methodology

In Table 6, three experimental factors, including HCl concentration (X_1), thiourea concentration (X_2), and O/A ratio (X_3) as well as the percentage of extraction (Y) were investigated. Such factors can be used to make predictions about the responses for the given levels of each factor. A quadratic polynomial model to predict percentage of arsenic extraction can be expressed as [40]:

$$Y = 27.816 + 29.757X_1 - 6.418X_2 - 5.84X_3 - 9.812X_1X_2 - 4.496X_1X_3 + 4.56X_2X_3 - 5.476X_1^2 - 59.759X_2^2 + 3.322X_3^2 \quad (10)$$

In Table 7, it was found that the correlation coefficient (R^2) was >0.9 , which indicated that the model was suitable to apply in the experiment. As for the Adjusted R^2 , when the Adjusted R^2 is >0.8 , this means that the relationship between the experimental and predicted results provided by the model is good [60]: the adequate precisions measure the signal-to-noise ratio. The Adequate Precision ratio of 12.01 indicates an adequate signal. Such a model can be used to navigate the design space [61]. The model F-value of 16.55 denotes the model is significant. There is only a 0.33 % chance that an F-value this large could occur due to noise. Moreover, P-values <0.05 indicate that the model terms are significant [53]. In Table 7, P-values demonstrate that X_2 (thiourea concentration), X_3 (O/A ratio), X_1X_3 (interaction between HCl concentration and O/A ratio), X_1^2 (self-interaction of HCl concentration), X_3^2 (self-interaction of O/A ratio) are significant model terms, which cannot be ignored.

In Fig. 6, response surface plots are shown for the best condition point to demonstrate the impact of HCl concentration (X_1), thiourea concentration (X_2), and O/A ratio (X_3) on the response variables. In Fig. 6(a), the surface plot at thiourea concentration is 0.02, thus percentage extraction increased when O/A ratio increased at low HCl concentration. Subsequently, percentage extraction decreased when O/A ratio increased at high HCl concentrations. However, the increase in both O/A ratio and HCl concentration are seen to generate high viscosity, which can cause poor contact between the condensate and extractant [59,62]. The interaction between the two parameters was significant. In Fig. 6(b), the interaction between HCl concentration and thiourea concentration was not significant. Likewise, in Fig. 6(c), the interaction between thiourea concentration and O/A ratio was not significant. Optimal conditions in the three parameters obtained via RSM are: 1 mol/L HCl concentration, 0.02 mol/L thiourea concentration and 4:1 O/A ratio.

3.5. Selectivity assessment

In Table 3, petroleum condensates containing arsenic, mercury, nickel, and zinc are shown. In Fig. 7, the synergistic extractant is seen to extract arsenic up to 56.4 % compared with other metals such as mercury (11.86 %), nickel (9.83 %), and zinc (0.17 %). The electronegativity of metals is in the following order: arsenic (2.18), mercury (2.00), nickel (1.91), and zinc (1.65). According to the highest electronegativity, arsenic has a higher efficiency to attend atoms in synergistic extractants than other metals [43]. It is acknowledged that the closer the separation factor is near to zero, two species are less likely to divide [42]. In Table 8, results demonstrate that the synergistic extractant has selective properties for the extraction of arsenic.

Table 5
Synergistic coefficients in various synergistic solutions.

Synergistic solutions	S
HCl + nitric acid	0.4605
HCl + methanol	0.5908
HCl + thiourea	1.4016

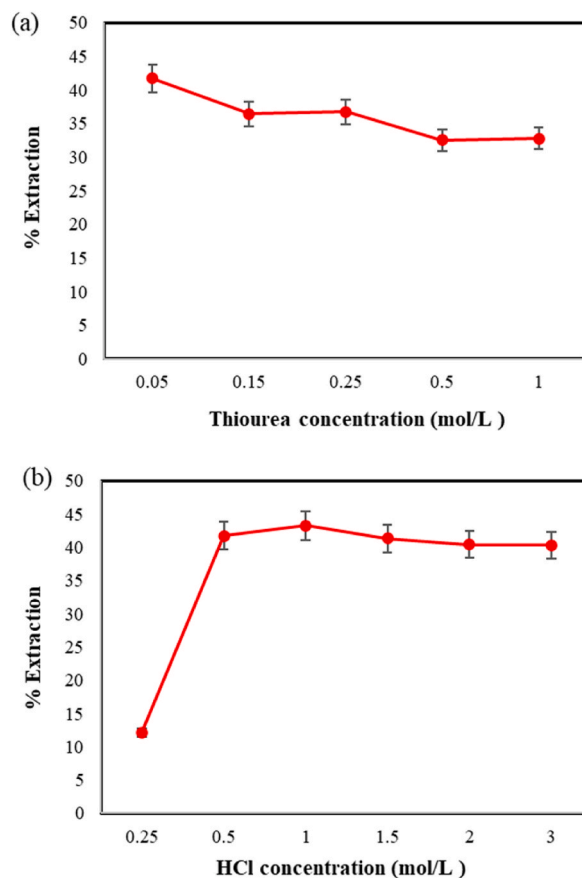


Fig. 5. (a) Percentages of extraction versus thiourea concentration: fixed HCl 0.5 mol/L, and (b) Percentages of arsenic removal versus HCl concentration: fixed thiourea 0.05 mol/L.

Table 6

The BBD method for three variables.

Standard order	X_1	X_2	X_3	% Extraction	
	HCl (mol/L)	Thiourea (mol/L)	O/A ratio	Experimental	Predicted
1	0.5	0.01	2.25	38.26	39.66
2	2.5	0.01	2.25	44.93	43.87
3	0.5	0.25	2.25	34.62	35.68
4	2.5	0.25	2.25	36.58	35.19
5	0.5	0.13	0.5	38.27	35.48
6	2.5	0.13	0.5	53.44	53.08
7	0.5	0.13	4	61.55	61.92
8	2.5	0.13	4	45.25	48.05
9	1.5	0.01	0.5	51.63	53.02
10	1.5	0.25	0.5	43.02	44.78
11	1.5	0.01	4	63.55	61.81
12	1.5	0.25	4	58.78	57.39
13	1.5	0.13	2.25	45.86	44.94
14	1.5	0.13	2.25	43.07	44.94
15	1.5	0.13	2.25	45.86	44.94

3.6. Effect of operating time on arsenic removal

In Fig. 8, during operating time, extraction percentage increased from 0 to 45 min; to reach equilibrium, arsenic extraction required 60 min. Thereby, the extraction of arsenic reached 56.4 %. Consequently, after 60 min, the percentage of arsenic was invariable, so operating time at 60 min was set up in the experiment.

Table 7
ANOVA for the quadratic model.

Source	DF	Adj SS	Adj MS	F-Value	P-Value
Model	9	1105.85	122.872	16.55	0.003
Linear	3	316.13	105.376	14.19	0.007
X_1	1	7.02	7.025	0.95	0.375
X_2	1	80.37	80.373	10.82	0.022
X_3	1	228.73	228.732	30.81	0.003
Square	3	532.87	177.623	23.92	0.002
$X_1^2X_1$	1	110.72	110.717	14.91	0.012
$X_2^2X_2$	1	2.73	2.734	0.37	0.57
$X_3^2X_3$	1	382.05	382.049	51.45	0.001
2-Way Interaction	3	256.85	85.618	11.53	0.011
$X_1^2X_2$	1	5.55	5.546	0.75	0.427
$X_1^2X_3$	1	247.64	247.641	33.35	0.002
$X_2^2X_3$	1	3.67	3.668	0.49	0.513
Error	5	37.13	7.425		
Lack-of-Fit	3	31.91	10.637	4.08	0.203
Pure Error	2	5.21	2.607		
Total	14	1142.98			
R^2		0.9675			
Adjusted R^2		0.9091			
Predicted R^2		0.543			
Adequate Precision		12.0101			

Note: DF = Degree of Freedom, Adj SS = Adjusted sums of squares, Adj MS = Adjusted mean squares.

3.7. Effect of temperature on arsenic removal

In Fig. 9, temperature is seen to be directly proportional to the percentages of extraction wherein the highest concentration of 78.2 % was obtained at 323.15 K. At high temperature, viscosity decreased, resulting in increased interaction between the organic phase and aqueous phase [59,63]. Energy is required to increase the reaction, which is a property of the endothermic reaction [24].

3.8. McCabe-Thiele plot

In Fig. 10, the McCabe-Thiele diagram is used to predict the number of extraction stages. As shown in Fig. 10, O/A ratio varied from 0.5:1–7:1, forming an equilibrium line. The equilibrium line can predict two-stage counter-current extraction enough for the required arsenic concentration (<0.01 mg/L) in petroleum condensate at 323.15 K and O/A ratio 4:1 as an operating line. In Table 9, batch simulation tests for two-stage counter-current extraction and estimation by McCabe-Thiele diagram are shown. As observed, extraction percentage reached 95.3 %. Subsequently, it was found that the error percentage between the McCabe-Thiele diagram and batch simulation was around 4 %.

3.9. Kinetics of arsenic removal from petroleum condensate

In Fig. 11, both integration and graphical techniques are used to define the reaction order and reaction rate constants. A linear plot was used to identify the slope and R^2 . In Table 10, the values for R^2 at each temperature for zero-order reaction was found to be more significant than the values for first-order and second-order reaction. Temperature is seen to affect the direct variation of the rate constants.

3.10. Activation energy

To determine the relationship between rate constant and activation energy, as a function of temperature, the linearized Arrhenius equation, as in Eq. (7) was applied. In Fig. 12, activation energy proved to be 217.88 kJ/mol. Activation energy >40 kJ/mol confirmed that chemical reaction is the rate-limiting step [64]. The Arrhenius equation of arsenic removal from petroleum condensate can be expressed as [43]:

$$k_{As} = 0.0878 \exp \left[\frac{-26.206}{T} \right] \quad (11)$$

3.11. Thermodynamics of arsenic removal from petroleum condensate

In Fig. 13, the thermodynamic parameters were evaluated according to Eq. (8). The thermodynamic parameters, which included ΔH° and ΔS° proved to be 46.19 kJ/mol and 0.15 kJ/mol•K, respectively. Moreover, the range of ΔG° from 303.15 to 323.15 K corresponded to the range of -0.47 to -3.55 kJ/mol. The positive value of ΔH° signifies that the reaction is endothermic, proving that extraction reaction increased when temperature increased [24]. The positive value of ΔS° indicated that extraction of arsenic in the

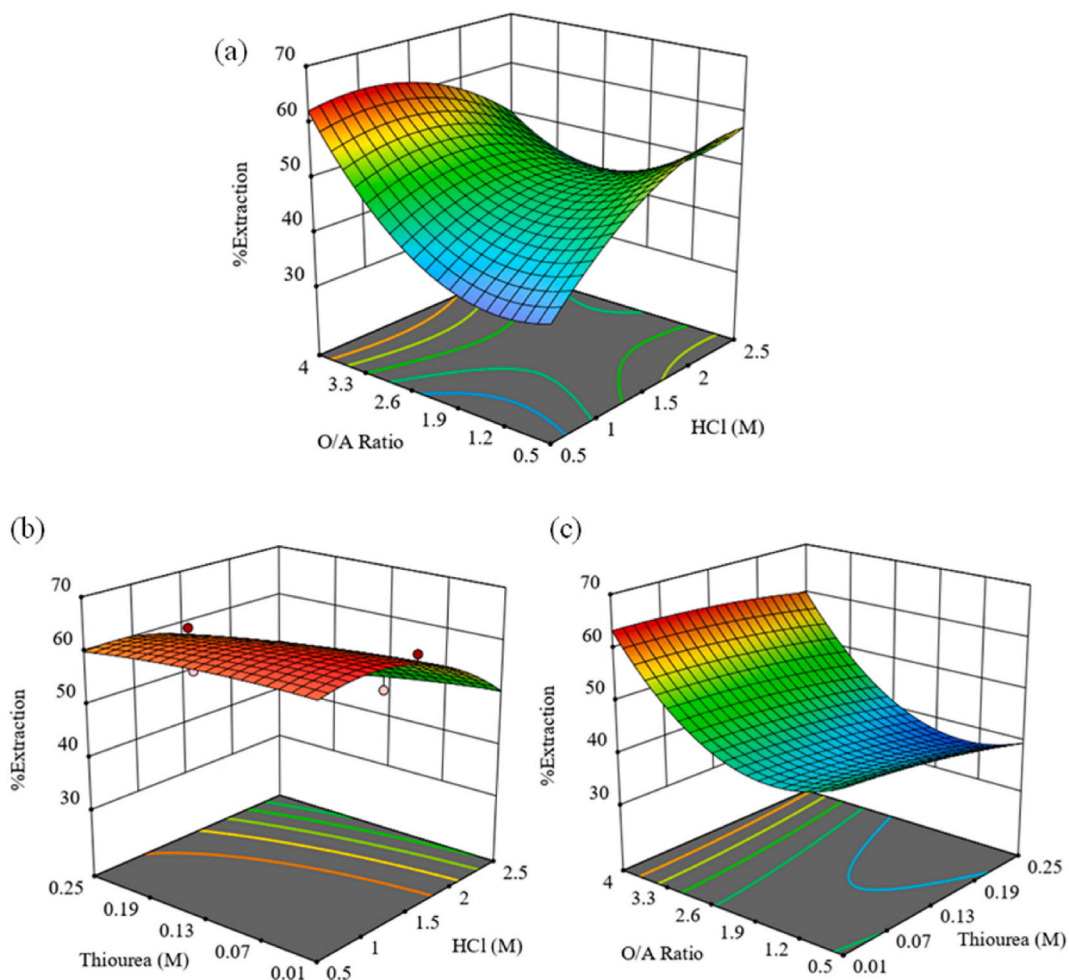


Fig. 6. 3D Response surface plots of the binary interactive effect: (a) HCl concentration and O/A ratio, (b) HCl concentration and thiourea concentration, and (c) Thiourea concentration and O/A ratio.

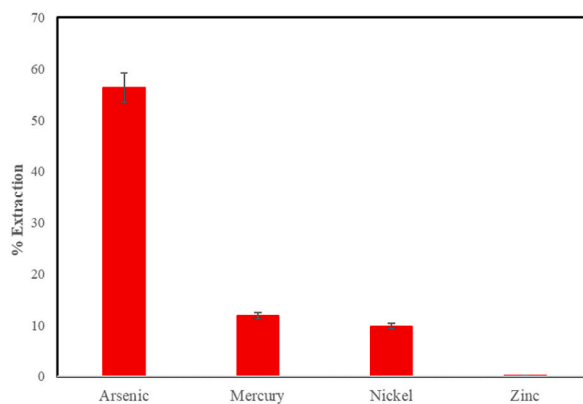


Fig. 7. Percentages of extraction versus metals in the petroleum condensate: HCl concentration = 1 mol/L, thiourea concentration = 0.02 mol/L, O/A ratio = 4:1, and T = 303.15 K.

Table 8
Separation factors of arsenic compared to other metals.

Separation factors	SF
$SF_{As,Hg}$	4.76
$SF_{As,Ni}$	5.74
$SF_{As,Zn}$	331.81

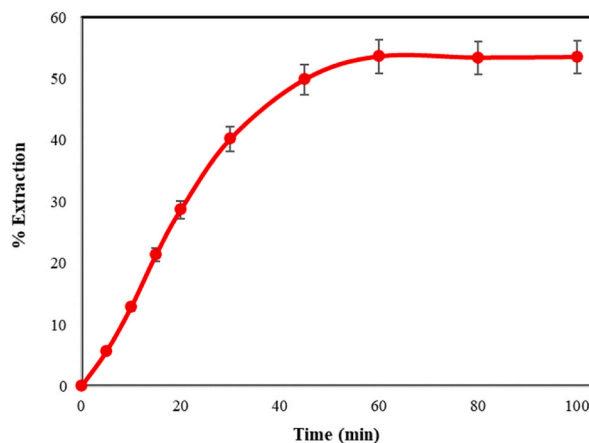


Fig. 8. Percentages of extraction versus time under conditions: HCl concentration = 1 mol/L, thiourea concentration = 0.02 mol/L, O/A ratio = 4:1, and T = 303.15 K.

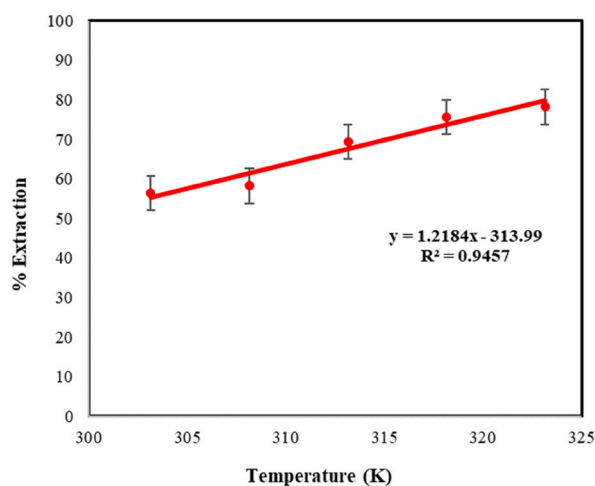


Fig. 9. Percentages of extraction versus temperature under conditions: HCl concentration = 1 mol/L, thiourea concentration = 0.02 mol/L for 60 min, O/A ratio = 4:1.

petroleum condensate is an irreversible reaction. In the case of ΔG° , its values were negative, implying that it is a feasible and spontaneous reaction: the extraction process was able to proceed [44,45].

3.12. DFT

3.12.1. Reaction mechanism of arsenic removal from petroleum

In Fig. 14, the mechanism for thiourea protonation by HCl at B3LYP/cc-pVDZ level of theory is shown. It is noted that when hydrochloric acid was added to thiourea in mol ratio 1:1, it resulted in protonation of the Sulphur atom in thiourea, thereby eliminating the chloride anion. This protonation affected the chemical bond length of C-S and the electrostatic potential in thiourea, which was in agreement with Traiwongsa et al. [65]. Consequently, the general structure of C-S is seen to have a high polarity property,

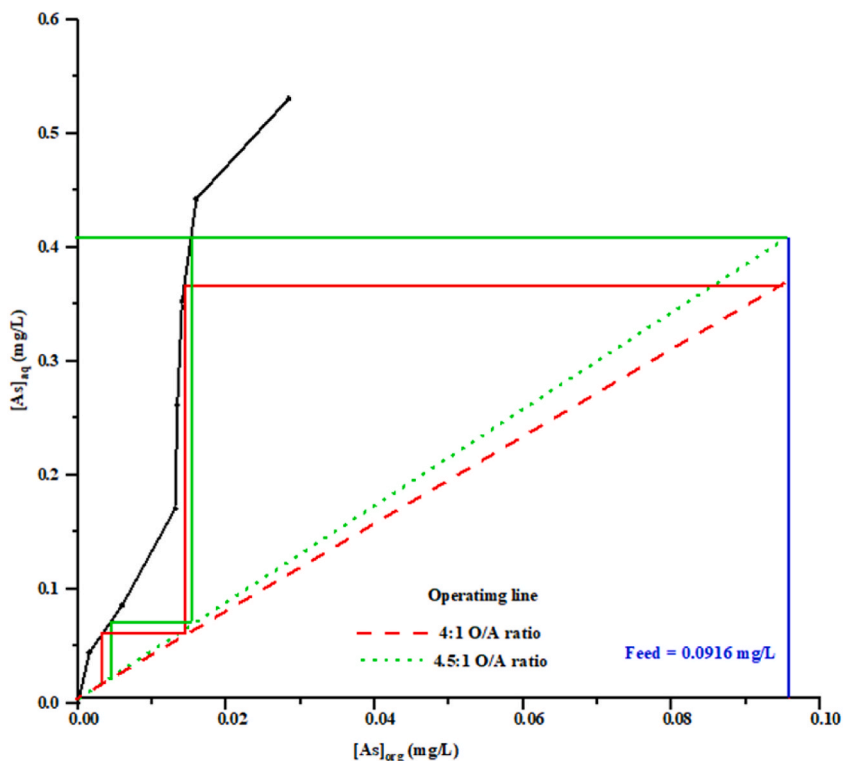


Fig. 10. McCabe-Thiele diagram under conditions: HCl concentration = 1 mol/L, thiourea concentration = 0.02 mol/L for 60 min and T = 323.15 K.

Table 9

Percentages of two-stage counter-current extraction.

Methods	Phase ratios (O/A)	% Extraction 1st stage	% Extraction 2nd stage
McCabe-Thiele diagram	4:1	84.5	96.8
	4.5:1	82.9	95.4
Batch simulation	4:1	80.4	95.3
	4.5:1	81.3	93.8

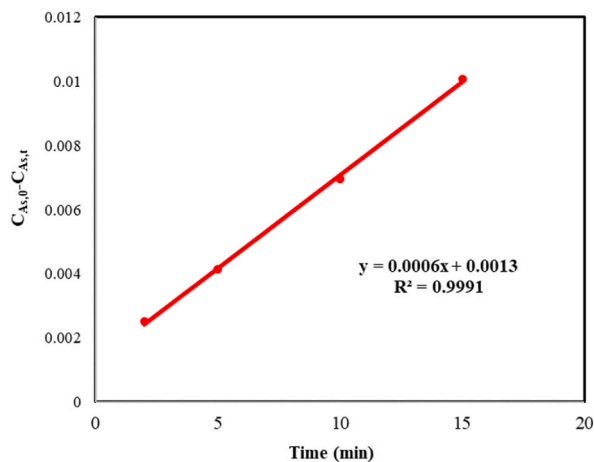


Fig. 11. Kinetics and rate constant of arsenic removal from petroleum condensate (zero order n = 0 and T = 303.15 K).

Table 10
Reaction order and rate constants of arsenic removal from petroleum condensate.

Reaction order	Linear plot	Temperature (K)	Rate constants	Unit	R ²
Zero order	$(C_{As,0} - C_{As,t})$ vs. t	303.15	0.0006	mg/L. min	0.9991
		313.15	0.0044		0.9598
		323.15	0.0060		0.9819
First order	$\ln(C_{As,0}/C_{As,t})$ vs. t	303.15	0.0062	min ⁻¹	0.9665
		313.15	0.0129		0.926
		323.15	0.0206		0.9245
Second order	$(1/C_{As,t}) - (1/C_{As,0})$ vs. t	303.15	0.0206	L/mg. min	0.9212
		313.15	0.2028		0.8951
		323.15	0.3851		0.9133

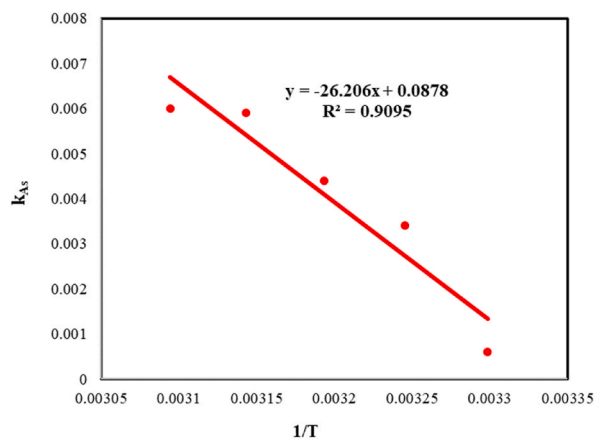


Fig. 12. The natural logarithm plot of the Arrhenius equation.

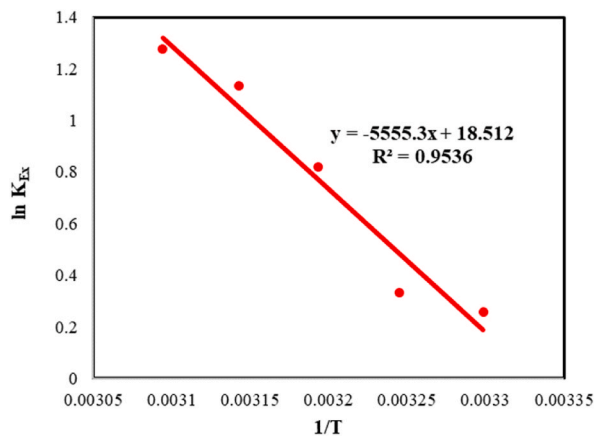


Fig. 13. Linear plots following the Van't Hoff equation under conditions: HCl concentration = 1 mol/L, Thiourea concentration = 0.02 mol/L for 60 min, O/A ratio = 4:1 at $T = 303.15$ – 323.15 K.

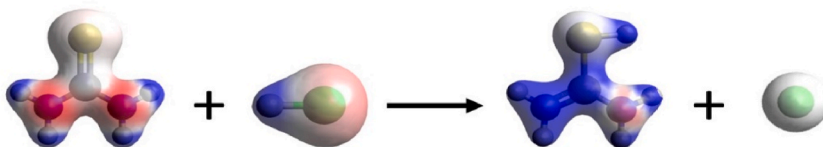


Fig. 14. The mechanism for thiourea protonation by HCl at B3LYP/cc-pVDZ level of theory.

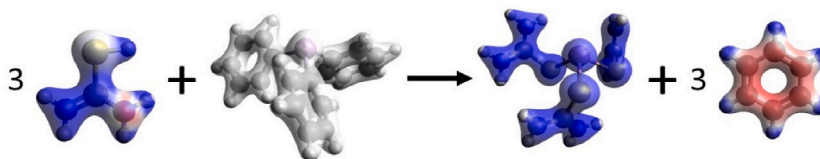


Fig. 15. The mechanism for protonated thiourea and $(C_6H_5)_3As$ at B3LYP/cc-pVDZ level of theory.

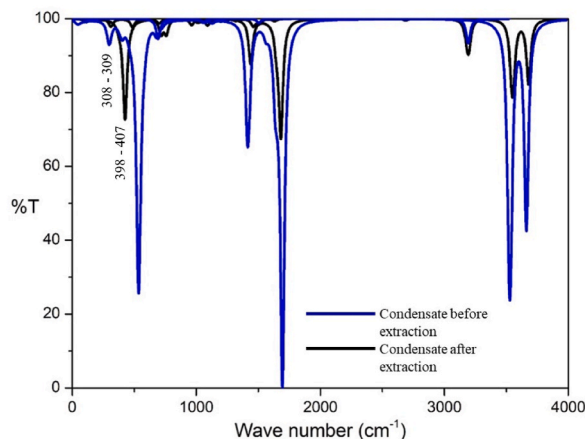


Fig. 16. Calculated IR spectra of condensate before and after the extraction at B3LYP/cc-pVDZ level of theory.

which means that the C–S bonding became weak because the ligand was a donation of C–S electrons to the metal center [26]. Moreover, the charge of the molecule on the thiourea protonate was found to be more positive (blue color) than thiourea. In Eq. (12), the chemical reaction of thiourea and hydrochloric acid is presented.



In Fig. 15, the mechanism for the three protonated thiourea and $(C_6H_5)_3As$ at B3LYP/cc-pVDZ level of theory is shown. It is noted that the lone pair electron of the Sulphur atom in the three protonated thiourea, forming the covalent bond with the arsenic atom in $(C_6H_5)_3As$, lost three protons to C_6H_5 . At the same time, As–C bonds are broken, resulting in the product of $(NH_2CSNH_2)_3As^{3+}$ and three C_6H_6 molecules. In Eq. (13), the reaction between the protonated thiourea and $(C_6H_5)_3As$ is presented:



3.12.2. Infrared spectroscopy

In Fig. 16, the calculated IR spectra of the condensate before and after extraction at B3LYP/cc-pVDZ level of theory are shown. The calculated IR vibrational spectra show the shift of the wave number of the arsenic vibrations. Before the reaction started, it was found that the vibrational frequencies of the arsenic in $(C_6H_5)_3As$ were in the range of 308–309 cm^{-1} due to the vibration of As–C bonds. Moreover, the form of arsenic in the condensate, as predicted by the computational quantum theory, agreed with FTIR calculations. After the reaction occurred, the vibrational frequencies of arsenic were observed and found to be in the range of 398–407 cm^{-1} . Such a shift was owing to the vibrations of As–S bonds in the $(NH_2CSNH_2)_3As^{3+}$ complex. The shift of the arsenic vibrations implied that the $(NH_2CSNH_2)_3As^{3+}$ complex occurred during the reaction. It is significant that the chemical bond strength of the As–S bond is greater than As–C bond.

4. Conclusions

In this work, results demonstrated that LLE using the synergistic extractant of HCl and thiourea could extract arsenic ions from petroleum condensate. It is significant that 0.050–2.100 mg/L of arsenic triphenylarsine ($(C_6H_5)_3As$) was successfully removed. Applying optimal conditions, percentages of extraction reached 78.2 %. Besides, the McCabe-Thiele method was able to estimate the two-stage counter-current extraction of arsenic to about 95.3 %. Thus, arsenic concentration was found to be lower than the limiting concentration of arsenic for use as feed to the furnace. The kinetics of the extraction process was discovered to be zero-order reaction. Moreover, thermodynamic analyses revealed that both ΔH° (46.19 kJ/mol) and ΔS° (0.15 kJ/mol·K) were positive but values of ΔG° were negative, indicating that the process was an endothermic reaction being irreversible and spontaneous. The mechanism of the extraction process was approved via DFT calculations.

Data availability statement

Data will be made available on request.

CRedit authorship contribution statement

Kittamuk Purktimatanont: Writing – original draft, Methodology, Investigation, Data curation. **Vanee Mohdee:** Writing – review & editing, Validation. **Ura Pancharoen:** Supervision, Funding acquisition, Conceptualization. **Kreangkrai Maneeintr:** Funding acquisition. **Wikorn Punyain:** Writing – review & editing, Software. **Anchaleeporn W. Lothongkum:** Writing – review & editing.

Declaration of competing interest

The authors declare that they have no known competing financial interests or personal relationships that could have appeared to influence the work reported in this paper.

Acknowledgements

The authors acknowledge the financial support from Thailand Science Research and Innovation Fund, Chulalongkorn University (IND6621005). Sincere thanks also go to the Separation Laboratory (Department of Chemical Engineering, Faculty of Engineering, Chulalongkorn University), and the National e-Science Infrastructure Consortium (NECTEC) for their contributions to this work.

References

- [1] F.d.S. Dias, et al., Application of multivariate techniques for optimization of direct method for determination of lead in naphtha and petroleum condensate by electrothermal atomic absorption spectrometry, *Mikrochim. Acta* 158 (3) (2007) 321–326.
- [2] M. Pyziur, *Condensate an Eprinc Primer*. Energy Policy Research Foundation, Energy Policy Research Foundation Inc, Washington, 2015.
- [3] A. Mere, et al., Arsenic analysis in the petroleum industry: a review, *ACS Omega* 7 (43) (2022) 38150–38157.
- [4] S. Chaturabul, et al., Arsenic removal from natural gas condensate using a pulsed sieve plate column and mass transfer efficiency, *Separ. Sci. Technol.* 47 (3) (2012) 432–439.
- [5] R. Güell, et al., Modelling of liquid–liquid extraction and liquid membrane separation of arsenic species in environmental matrices, *Sep. Purif. Technol.* 72 (3) (2010) 319–325.
- [6] R.J. Cassella, O.D. Sant’Ana, R.E. Santelli, Determination of arsenic in petroleum refinery streams by electrothermal atomic absorption spectrometry after multivariate optimization based on Doehlert design, *Spectrochim. Acta B: At. Spectrosc.* 57 (12) (2002) 1967–1978.
- [7] V. Mohdee, et al., Synergistic interplay between Aliquat 336 and organophosphorus extractants towards non-dispersive extraction of arsenic from petroleum produced water via hollow fiber membrane contactor, *Sep. Purif. Technol.* 286 (2022), 120431.
- [8] M.V. Reboucas, S.L.C. Ferreira, B. Barros Neto, Behaviour of chemical modifiers in the determination of arsenic by electrothermal atomic absorption spectrometry in petroleum products, *Talanta* 67 (1) (2005) 195–204.
- [9] S. Ichikawa, et al., Process for Removing Arsenic from a Petroleum Fraction, European Patent, 1989, 0270675.
- [10] C.G. Brown, L.G. Sherrington, Solvent extraction used in industrial separation of rare earths, *J. Chem. Technol. Biotechnol.* 29 (4) (1979) 193–209.
- [11] G. Bacon, I. Mihaylov, Solvent extraction as an enabling technology in the nickel industry, *J. South. Afr. Inst. Min. Metall.* 102 (8) (2002) 435–443.
- [12] P.M. Cole, K.C. Sole, Zinc solvent extraction in the process industries, *Miner. Process. Extr. Metall. Rev.* 24 (2) (2003) 91–137.
- [13] A. Schmidt, J. Strube, in: Kirk-Othmer (Ed.), *Application and Fundamentals of Liquid–Liquid Extraction Processes: Purification of Biologicals, Botanicals, and Strategic Metals*, fifth ed. Kirk-Othmer Encyclopedia of Chemical Technology, John Wiley & Sons, New York, 2018, pp. 1–52.
- [14] A. Khatibi, S. Hamidi, M. Siah-Shadbad, Application of liquid-liquid extraction for the determination of antibiotics in the foodstuff: recent trends and developments, *Crit. Rev. Anal. Chem.* 52 (2020) 1–16.
- [15] A. Sridhar, et al., Extraction techniques in food industry: insights into process parameters and their optimization, *Food Chem. Toxicol.* 166 (2022), 113207.
- [16] L. Tavlarides, J. Bae, C. Lee, Solvent extraction, membranes, and ion exchange in hydrometallurgical dilute metals separation, *Separ. Sci. Technol.* 22 (2–3) (1987) 581–617.
- [17] V.J. Inglezakis, S.G. Pouloupoulos, in: V.J. Inglezakis, S.G. Pouloupoulos (Eds.), *Adsorption, Ion Exchange and Catalysis: Design of Operations and Environmental Applications*, first ed. Adsorption, Ion Exchange and Catalysis: Design of Operations and Environmental Applications, Elsevier, Amsterdam, 2006.
- [18] J. Rydberg, M. Cox, Solvent extraction principles and practice, revised and expanded, in: J. Rydberg (Ed.), *Solvent Extraction Principles and Practice, Revised and Expanded*, second ed., CRC press, Florida, 2004.
- [19] W.L. McCabe, J.C. Smith, P. Harriott, *Unit Operations of Chemical Engineering*, sixth ed., McGraw Hill, New York, 2001.
- [20] J. Yao, et al., Extraction of chloride from slag flush wastewater using solvent N235, *Hydrometallurgy* 213 (2022), 105934.
- [21] M. Kasaie, H. Bahmanyar, M.A. Moosavian, A kinetic study on solvent extraction of copper from sulfate solution with Cupromex-3302 using Lewis cell, *J. Environ. Chem. Eng.* 5 (3) (2017) 3044–3050.
- [22] R. Torkaman, et al., A kinetic study on solvent extraction of samarium from nitrate solution with D2EHPA and Cyanex 301 by the single drop technique, *Hydrometallurgy* 150 (2014) 123–129.
- [23] P. Skrzypczyk, A.J. Short, S. Popescu, Work extraction and thermodynamics for individual quantum systems, *Nat. Commun.* 5 (1) (2014) 4185.
- [24] M.D. Koretsky, *Engineering and Chemical Thermodynamics*, second ed., John Wiley & Sons, Inc, New York, 2012.
- [25] D.E. Ellis, in: *Density Functional Theory of Molecules, Clusters, and Solids*. First Ed, Ed. D. Ellis, Vol. 12, Kluwer Academic, Dordrecht, 1995.
- [26] V. Mohdee, V. Parasuk, U. Pancharoen, Synergistic effect of Thiourea and HCl on Palladium (II) recovery: an investigation on Chemical structures and thermodynamic stability via DFT, *Arab. J. Chem.* 14 (7) (2021), 103196.
- [27] C. Venkateswara Rao, et al., Anion assisted extraction of U(VI) in alkylammonium ionic liquid: experimental and DFT studies, *Sep. Purif. Technol.* 261 (2021), 118275.
- [28] P.J. Stephens, et al., Ab initio calculation of vibrational absorption and circular dichroism spectra using density functional force fields, *J. Phys. Chem.* 98 (45) (1994) 11623–11627.
- [29] J. Kullgren, et al., B3LYP calculations of cerium oxides, *J. Chem. Phys.* 132 (5) (2010), 054110.
- [30] Q. Sun, H. Chen, J. Yu, A DFT investigation of the lithium extraction process under different diluent environments, *Chem. Eng. Sci.* 277 (2023), 118857.
- [31] P.N. Khan, P. Sinharoy, A. Bhattacharyya, Experimental and theoretical studies (DFT) on technetium extraction as HTcO4 using dicyclohexano-18-crown-6 in a blend of isodecyl alcohol and n-dodecane from acidic medium, *Prog. Nucl. Energy* 160 (2023), 104684.
- [32] M. Wisniewski, Extraction of arsenic from sulphuric acid solutions by Cyanex 923, *Hydrometallurgy* 46 (1) (1997) 235–241.

- [33] U. Pancharoen, W. Poonkum, A.W. Lothongkum, Treatment of arsenic ions from produced water through hollow fiber supported liquid membrane, *J. Alloys Compd.* 482 (1) (2009) 328–334.
- [34] N. Jantunen, et al., Removal and recovery of arsenic from concentrated sulfuric acid by solvent extraction, *Hydrometallurgy* 187 (2019) 101–112.
- [35] S. Suren, et al., The elimination of trace arsenic via hollow fiber supported liquid membrane: experiment and mathematical model, *Sci. Rep.* 11 (1) (2021), 11790.
- [36] L. Zeng, et al., Removal and recovery of arsenic(III) from hydrochloric acid leach liquor of tungsten slag by solvent extraction with 2-ethylhexanol, *J. Miner. Met. Mater. Soc.* 74 (8) (2022) 3021–3029.
- [37] A. Ahmad, et al., Box-behnken response surface design of polysaccharide extraction from *Rhododendron arboreum* and the evaluation of its antioxidant potential, *Molecules* 25 (17) (2020).
- [38] S. Roy, et al., Optimization of turmeric oil extraction in an annular supercritical fluid extractor by comparing BBD-RSM and FCCD-RSM approaches, *Mater. Today: Proc.* 76 (2023) 47–55.
- [39] V. Mohdee, et al., Optimization of process parameters using response surface methodology for Pd(II) extraction with quaternary ammonium salt from chloride medium: kinetic and thermodynamics study, *Chem. Pap.* 72 (12) (2018) 3129–3139.
- [40] K. Aziz, et al., Enhanced biosorption of bisphenol A from wastewater using hydroxyapatite elaborated from fish scales and camel bone meal: a RSM@BBD optimization approach, *Ceram. Int.* 48 (11) (2022) 15811–15823.
- [41] W. Poolkaew, et al., New upstream solution for mercury removal from petroleum condensate via HFMC: thermodynamics, kinetics, DFT and mass transport, *Hydrometallurgy* 221 (2023), 106135.
- [42] K. Rezaei, H. Nedjate, Diluent effect on the distribution ratio and separation factor of Ni(II) in the liquid–liquid extraction from aqueous acidic solutions using dibutylthiophosphoric acid, *Hydrometallurgy* 68 (1) (2003) 11–21.
- [43] T. Wongsawa, et al., New and green extraction of mercury(I) by pure sunflower oil: mechanism, kinetics and thermodynamics, *J. Taiwan Inst. Chem. Eng.* 122 (2021) 40–50.
- [44] T. Pirom, et al., The effect of temperature on mass transfer and thermodynamic parameters in the removal of amoxicillin via hollow fiber supported liquid membrane, *Chem. Eng. J.* 265 (2015) 75–83.
- [45] M.D. Kostić, et al., The kinetics and thermodynamics of hempseed oil extraction by n-hexane, *Ind. Crops Prod.* 52 (2014) 679–686.
- [46] J.L.A. Dagostin, D. Carpiné, M.L. Corazza, Extraction of soybean oil using ethanol and mixtures with alkyl esters (biodiesel) as co-solvent: kinetics and thermodynamics, *Ind. Crops Prod.* 74 (2015) 69–75.
- [47] M. Frisch, et al., Gaussian 09, Revision D. 01, Gaussian, Inc, Wallingford, 2009.
- [48] M.D. Hanwell, et al., Avogadro: an advanced semantic chemical editor, visualization, and analysis platform, *J. Cheminf.* 4 (1) (2012) 17.
- [49] A.R. Allouche, Gabetit—a graphical user interface for computational chemistry softwares, *J. Comput. Chem.* 32 (1) (2011) 174–182.
- [50] A. Winter, *Organic Chemistry I for Dummies*, Wiley, New York, 2016.
- [51] D. Behera, B.K. Nandi, S. Bhattacharya, Variations in combustion properties of coal with average relative density and functional groups identified by FTIR analysis, *Int. J. Coal Prep. Util.* 42 (6) (2022) 1695–1711.
- [52] R.M. Giuliano, A. Francis, D. Carey, *Organic Chemistry*. Tenth Ed. Carey, D, McGraw-Hill Education, New York, 2016.
- [53] K. Duangchan, et al., Mercury elimination from synthetic petroleum produced water using green solvent via liquid–liquid extraction: experimental, effective solubility behaviors and DFT investigation, *J. Environ. Chem. Eng.* 11 (2) (2023), 109296.
- [54] S. Suren, et al., Uphill transport and mathematical model of Pb(II) from dilute synthetic lead-containing solutions across hollow fiber supported liquid membrane, *Chem. Eng. J.* 191 (2012) 503–511.
- [55] V. Mohdee, et al., Synergistic strippants of Pd (II) ions in the presence of chloride medium from wastewater of electroless plating process via solvating system: kinetics and thermodynamics study, *Separ. Sci. Technol.* 54 (17) (2019) 2971–2982.
- [56] Y. Luo, *Comprehensive Handbook of Chemical Bond Energies*, first ed., CRC press, Florida, 2007.
- [57] J.G. Calvert, Glossary of atmospheric chemistry terms (Recommendations 1990), *Pure Appl. Chem.* 62 (11) (1990) 2167–2219.
- [58] J. Stas, H. Alsawaf, Liquid–liquid extraction of hydrochloric acid from aqueous solutions by tri-n-dodecylamine and tri-n-octylamine/diluents, *Period. Polytech. - Chem. Eng.* 60 (2) (2016) 130–135.
- [59] L. Zhang, et al., Purification of chlorine-containing wastewater using solvent extraction, *J. Clean. Prod.* 273 (2020), 122863.
- [60] K. Aziz, et al., Engineering of highly Brachycton populneus shells@polyaniline bio-sorbent for efficient removal of pesticides from wastewater: optimization using BBD-RSM approach, *J. Mol. Liq.* 346 (2022), 117092.
- [61] C.F.Z. Lacson, M.-C. Lu, Y.-H. Huang, Calcium-based seeded precipitation for simultaneous removal of fluoride and phosphate: its optimization using BBD-RSM and defluoridation mechanism, *J. Water Process Eng.* 47 (2022), 102658.
- [62] K.L. Wasewar, et al., Fermentation of glucose to lactic acid coupled with reactive extraction: a review, *Ind. Eng. Chem. Res.* 43 (19) (2004) 5969–5982.
- [63] J.F.P. Bassane, et al., Study of the effect of temperature and gas condensate addition on the viscosity of heavy oils, *J. Pet. Sci. Eng.* 142 (2016) 163–169.
- [64] V.S. Kislík, in: V.S. Kislík (Ed.), *Liquid Membranes: Principles and Applications in Chemical Separations and Wastewater Treatment*, first ed. Liquid Membranes: Principles and Applications in Chemical Separations and Wastewater Treatment, Elsevier, Amsterdam, 2010, pp. 17–71.
- [65] N. Traiwongsa, et al., Mechanisms of mercury ions separation by non-toxic organic liquid membrane via DFT, thermodynamics, kinetics and mass transfer model, *J. Ind. Eng. Chem.* 117 (2023) 522–537.